

The Development of Strong Acidity in Hexafluorosilicate-Modified Y-Type Zeolites

FERENC LÓNYI¹ AND JACK H. LUNSFORD²

Department of Chemistry, Texas A&M University, College Station, Texas 77843

Received December 30, 1991; revised March 19, 1992

Catalysts have been prepared by treating a parent Na,NH₄-Y(54) zeolite containing 54 Al_f/u.c. with ammonium hexafluorosilicate (AHFS). The resulting zeolites, containing between 39 and 26 Al_f/u.c., were crystalline, but were relatively inactive for the cracking of *n*-hexane at 400°C. After steaming they became active, and their activity was greater than that of a parent zeolite which had been steamed to the same framework aluminum (Al_f) content. To achieve maximum activity by steaming the amount of Al removed from the AHFS-treated zeolite was equivalent to ca. one Al atom per β cage. The enhanced activity of the steamed AHFS-treated material is believed to result from the presence of isolated Al in the framework and a cationic form of extraframework Al in the β cages. It is apparent from the ²⁹Si NMR spectrum that the resonance of Si atoms connected to three Al_f atoms is not present in the AHFS-treated samples. The absence of this ²⁹Si resonance is consistent with an increase in isolated Al_f atoms. All of the zeolites contained an octahedral form of extraframework Al which has no effect on acidity or activity. The most active zeolites are characterized by infrared bands at 3602 and 3525 cm⁻¹, which are assigned to hydroxyl groups in the large and small cages, respectively. The zeolites prepared with AHFS retained less than 0.3 wt% fluorine. It is unlikely that this fluorine is responsible for the enhanced acidity of the more active catalysts. Impregnation of the less active catalysts with NH₄F increased the activity; however, this phenomenon results from dealumination rather than from the electronic effect of fluorine.

© 1992 Academic Press, Inc.

INTRODUCTION

It is now evident that a normal H-Y zeolite, with its full complement of protons, is a relatively inactive catalyst for such hydrocarbon reactions as cumene dealkylation and hexane cracking (1–3). If this material is steamed or treated with SiCl₄, aluminum is removed from the framework and deposited in several possible forms in the cavities of the zeolite. In addition, the activity for acid-catalyzed reactions increases up to a maximum level at ca. 32 framework aluminum atoms (Al_f) per unit cell (u.c.). Upon further dealumination the activity decreases linearly with respect to Al_f content.

¹ On leave from the Central Research Institute of Chemistry of the Hungarian Academy of Sciences, P.O. Box 17, H-1525 Budapest, Hungary.

² To whom correspondence should be addressed.

In order to understand the mechanism by which dealumination enhances catalytic activity, one would like to be able to separate the roles of Al_f distribution and the effect of extraframework Al species. This has been achieved, in part, by studying the activity of an H-ZSM-20 zeolite which contained 41 Al_f/u.c., but no extraframework Al (4). ZSM-20 is an intergrowth of the cubic faujasite (FAU) structure and a hexagonal form known as Breck structure six (BSS). The particular ZSM-20 zeolite used in the activity study had a ratio of FAU-to-BSS of approximately 1.8. If the Al_f distribution were the only factor in effecting strong acidity, one would expect this material to be highly active for hexane cracking, but, in fact, it exhibited very little activity (3, 4).

It is possible to produce Y-type zeolites having ca. 30–40 Al_f/u.c., but a limited amount of extraframework Al, by treating a

normal zeolite Y (Si/Al = 2.5) with ammonium hexafluorosilicate (AHFS). This method was first reported by Skeels and Breck (5). As a part of a broader study on the effects of dealumination, Beyerlein *et al.* (6) showed that a zeolite modified by AHFS had relative little activity for acid-catalyzed isobutane cracking, but the activity became greater when the sample was subsequently steamed. The activity was even greater than that of conventionally steamed sample that had the same Al_f concentration. Similarly, a commercial form of this catalyst (Union Carbide LZ-210) which had been steamed was found to be active in a MAT test (7). We have shown that Y-type zeolites treated with AHFS are inactive for hexane cracking (3).

Several theories have been proposed to explain the interplay between framework and extraframework aluminum in creating strong acidity in zeolites Y, ZSM-20, and ZSM-5. These have recently been summarized (4). We have proposed that two requirements are essential for strong acidity: (i) there must be only one Al_f atom in a four-ring of the zeolite, and (ii) the β -cage must contain aluminum cations. In the present study this hypothesis was further tested using a series of Y-type zeolites dealuminated with AHFS. These materials were subsequently steamed to achieve differing amounts of extraframework Al. The activities of the catalytic materials for hexane cracking were compared with those of Y-type zeolites that had been dealuminated using conventional steaming. The zeolites were characterized by a number of techniques including solid-state NMR. In addition to the roles of framework and extraframework Al, the significance of residual fluorine in the catalyst also was evaluated.

EXPERIMENTAL

Catalyst Preparation

Four different zeolites were prepared by AHFS modification of the parent Na, NH_4 -Y-zeolite, provided by Union Carbide,

which contained 54 Al_f /u.c. These samples were then mildly or severely steamed. Several steamed samples also were prepared from the parent Y-zeolite for comparison.

Zeolites dealuminated with AHFS were prepared using a variation of the method of Skeels and Breck (5). A 40-g sample of the zeolite was slurried in 400 ml of deionized water and heated between 80 and 90°C. To this slurry a 1 M solution of AHFS was added with stirring at a rate of 0.005 mol reactant per mol aluminum per minute. The total amount of solution added depended on the desired degree of dealumination; the calculated amount of Al, based on stoichiometry, generally was extracted. The resultant slurry was maintained at 80–90°C for 3 h with stirring, then filtered while hot and washed with 1 liter of hot water four times to remove fluorides.

The mild or severe steaming was carried out in a fused quartz reactor tube at 550°C for 1 h or at 600°C for 3 h, respectively. An N_2 /steam mixture saturated with H_2O at 85°C (415 Torr of water) was passed over 6 g of zeolite at a flow rate of 30 ml/min. The temperature was raised gradually (5°C/min) to the final dealumination temperature. The N_2 /steam flow rate was increased and/or a higher temperature (650°C) was used in some cases in order to increase the extent of dealumination. Finally, the zeolite was cooled in the N_2 /steam mixture and dried at 120°C in flowing N_2 .

The samples were transformed to the ammonium form by ion exchanging 5–10 g of the zeolite in 1 liter of 1 M NH_4NO_3 solution at 70°C for 2 h with stirring. The zeolite was filtered, washed with 1 liter of deionized water, and dried at 100°C. This procedure was repeated three times. The extent of ion-exchange was greater than 99% (less than 0.03 wt% of Na) in every case.

Fluorine was purposely introduced by an incipient wetness technique in which 1 ml of 0.1 M NH_4F solution was added to 0.5 g of zeolite. After 24 h the sample was dried overnight at 120°C.

Evaluation of Catalytic Activity

Catalytic measurements were carried out in a fused-quartz flow reactor having an internal diameter of 5 mm. A stream of N₂ (20 ml/min) was passed through a n-hexane saturator at 0°C and then into the catalytic reactor. A 42–45 mg sample of catalyst (20–45 mesh) was placed on quartz wool. The upper part of the reactor was packed with quartz chips to preheat the reactant gases. The samples were activated *in situ* by heating under flowing N₂ for 1 h at 100°C, 40 min at 200 and 300°C each, and then 2 h at 400°C. The reaction temperature was 400°C in every run. A sample was taken after 5 min on stream. The *n*-hexane conversion was determined by GC product analysis (C₁–C₆ hydrocarbons) using a Carle III chromatograph equipped with a 3-m Porapak Q (80–100 mesh) column at 150°C. The activity was calculated from the amount of products obtained. The maximum conversion in these experiments was 27%; the range of conversion was 0.8–27%.

Characterization

A total analysis of the zeolites was carried out by dissolving the samples in a solution of hydrofluoric acid and perchloric acid. The solution was heated on a hot plate until the liquid had completely evaporated, and the residue was then dissolved in water. The resulting solution was analyzed for Na⁺ and Al³⁺ by the ion-coupled plasma method (ICP), using an ARL 3510 ICP spectrometer. The error in this analysis is estimated to be ±1 Al/u.c.

The fluorine content of the zeolites was determined by using a fluorine selective electrode and a "known addition" technique (8). The zeolite sample was decomposed by using an Na₂CO₃–K₂CO₃ melt at 1000°C. After cooling, the mixture was dissolved in an aqueous HCl solution. The fluoride ion concentration was calculated from the difference of the electrode potentials measured before and after addition of a known amount of standard NaF solution.

The zeolite samples were checked by X-ray diffraction for crystallinity, and the unit cell parameter was determined relative to Pb(NO₃)₂ ($a_0 = 7.8568 \text{ \AA}$) (9). The X-ray diffraction patterns were obtained with a Seifert–Santag Pad II automated diffractometer. The percent crystallinity values were obtained according to the ASTM D 3906-85a method.

Infrared spectra were measured at 2 cm⁻¹ nominal resolution on a Perkin–Elmer 1710 FTIR spectrometer equipped with a high-sensitivity MCT detector. The zeolite samples were pretreated in N₂ flow under the same conditions as the catalytic samples and then were pressed into self-supporting wafers (6–8 mg/cm²). The zeolite wafer was heated up to 400°C under vacuum (10⁻⁵ Torr) at a rate of 0.6°C/min and was kept at 400°C for 4 h. After recording the spectrum at room temperature, 5 Torr of pyridine vapor was introduced into the cell and allowed to react with the zeolite wafer for 30 min. The cell was evacuated at 250°C for 4 h to eliminate the weakly adsorbed pyridine and cooled to room temperature for recording a second spectrum. A third spectrum was recorded after the same procedure, except the cell was evacuated at 400°C for 4 h.

The ²⁹Si and ²⁷Al spectra were obtained using a Bruker MSL-300 spectrometer (7.05 T). About 0.2 g of hydrated zeolite was loaded into a zirconium rotor and spun (3 kHz) at the magic angle to remove line broadening caused by homonuclear or heteronuclear interactions. ²⁹Si or ²⁷Al spectra were obtained after 1200–5200 or 800–1600 accumulations, respectively. The Si/Al ratio was calculated using the method of Engelhardt *et al.* (10). An error of approximately ±1 Al_f/u.c. is estimated.

RESULTS

Catalyst Characterization

The zeolite samples prepared by AHFS dealumination (Y(39)–Y(26)) had good crystallinity except the sample Y(26), for which more than 50% loss in crystallinity was observed. The Al_f/u.c. content of 28 is appar-

TABLE 1
Analysis of Zeolite Samples

Zeolite	a_0	Total Al/u.c. (ICP)	Al _f /u.c. (²⁹ Si NMR)	Crystallinity (%)
Y(39) ^a	24.593	36	39	97
Y(30)	—	27	30	—
Y(28)	24.508	26	28	91
Y(26)	24.414	17	26	45
smY(39) ^b	24.533	—	34	100
smY(28)	24.426	25	26	108
smY(30)	—	—	24	—
smY(26)	24.368	—	23	53
ssY(39)-1 ^c	24.533	—	29	106
ssY(39)-2	—	—	26	—
ssY(39)-3	—	—	18	—
ssY(28)	24.410	25	20	110
ssY(30)-1	—	—	16	—
ssY(30)-2	—	—	13	—
ssY(26)	24.368	—	20	50
Y(54) ^d	24.742	—	54	100
smY(54) ^e	24.676	—	43	82
ssY(54)-1 ^f	24.589	—	38	89
ssY(54)-2	—	—	32	—
ssY(54)-3	—	—	29	—
ssY(54)-4	—	54	27	—
ssY(54)-5	—	53	21	—

^a Prepared from the parent Y(54) zeolite by AHSF treatment.

^b AHSF treated series after mild steaming.

^c AHSF treated series after severe steaming.

^d Parent zeolite.

^e Mild steamed parent zeolite.

^f Severely steamed parent zeolite series.

ently the lower limit for dealumination of a Y-type zeolite with AHFS in a single step if one wants to retain good crystallinity.

The unit cell constant, the total Al content, the framework Al content, and the crystallinity of the zeolites used in this study are listed in Table 1. The numbers given in parenthesis refer to the Al_f/u.c. for the respective zeolite. The parent material, Y(54) was assigned a crystallinity of 100%. The total Al content and the framework Al content decreased in a parallel manner, and (except for Y(26)) the Al contents obtained by the two methods were nearly equivalent. In fact, the value for Al_f/u.c. was somewhat greater than the value for the total Al/u.c. This difference reflects the errors in analyses. By contrast both mild and severely steamed samples retained most of the Al which was originally in the zeolite.

The fluorine contents of the zeolite sam-

ples are listed in Table 2. The Y(39) zeolite, which contained the least amount of fluorine after preparation, lost the least amount of fluorine upon steaming. The Y(28) and Y(26) zeolites lost approximately half of their fluorine upon steaming. The fluorine introduced to the mildly steamed parent catalyst (0.35 wt%) was largely retained in the zeolite after activation.

Activity for *n*-Hexane Cracking

As can be seen in Fig. 1 the parent zeolite and the samples prepared by AHFS modification had little activity for hexane cracking in their pure H-form. It was noted previously that the activity of samples prepared by steaming the parent Y(54) zeolite increased almost linearly with respect to Al_f concentration, up to ca. 32 Al_f/u.c., and then decreased to zero (extrapolated) at ca. 64 Al_f/u.c. (1, 2, 6). The line through the solid squares in Fig. 1 is the functional relationship for Al_f atoms having no next-nearest neighbors in the zeolite four-rings. This relationship was derived from the statistical model of Beagley *et al.* (11), assuming repulsive interactions between aluminum tetrahedra. We and others have shown that the linear relationship between activity and

TABLE 2

Fluorine Content of Zeolite Samples

Zeolite	Fluorine content (wt%)
Y(39) ^a	0.15
Y(28)	0.28
Y(26)	0.62
smY(39) ^b	0.15
ssY(39)-1	0.13
smY(28)	0.14
ssY(28)	0.19
smY(28)	0.26
ssY(28)	0.27
smY(54)/F ^c	0.33

^a As prepared by AHSF treatment.

^b After mild or severe steaming.

^c Mild steamed parent zeolite after fluorine treatment and activation in nitrogen at 400°C.

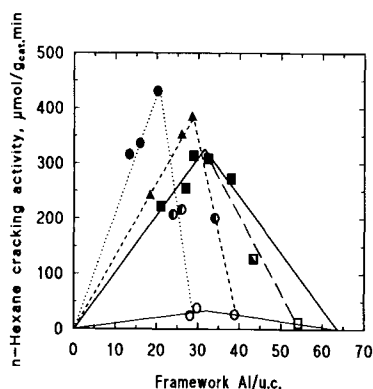


FIG. 1. Dependence of hexane cracking activity on framework Al content at 400°C: □, parent zeolite; ◻, mildly steamed parent catalyst; ◼, severely steamed parent catalyst; ○, AHFS-modified series; ●, AHFS-modified series after mild steaming; ●, ▲, AHFS-modified series after severe steaming.

Al_f/u.c. may be extended to quite small aluminum contents (1, 2, 11). The lower Al_f concentrations were achieved either by treatment of the zeolite by SiCl₄ (1, 2) or by steaming the zeolite, followed by more extensive dealumination with HCl (1). In each case the activity data could be represented by a single straight line.

By contrast the activity of each zeolite prepared with AHFS, followed by steaming, had a unique functional relationship. Moreover, the maximum activity, which occurred at <32 Al_f/u.c., was greater than the maximum activity that could be achieved in the steamed Y(54) sample. In agreement with the results of Beyerlein *et al.* (6) the activity of a zeolite dealuminated with AHFS to about 30 Al_f/u.c. and steamed to 20 Al_f/u.c. was considerably greater than the activity of a catalyst that had only been steamed to about 20 Al_f/u.c.

The amount of extraframework Al needed to reach the maximum activity of an AHFS-treated sample was only 8 to 10 Al_f/u.c. Furthermore, the increase in activity, up to the maximum, appears to be linear with respect to the amount of extraframework Al. These results agree with those obtained previously with a steamed ZSM-20 zeolite (4).

The effect of fluorine treatment on the activity of several catalyst samples is shown in Table 3. The activity of the catalysts increased some extent in every case after fluorine treatment; however, with the more active catalysts the percentage increase was small. Parallel to the activity increase, a slight framework dealumination was detected in two of the steamed parent zeolite samples by ²⁹Si NMR (and also by an IR spectroscopic investigation of the pyridine adsorbed on Lewis acidic sites—spectra not shown) after fluorine treatment and activation at 400°C in N₂ flow. Probably a similar dealumination step occurred in the normal Y-zeolite and the other unsteamed zeolites which resulted in an activity increase. In the severely steamed AHFS-modified samples, where the Al_f content was below 30 Al_f/u.c. and more severe conditions are necessary for further dealumination, the activities increased only slightly after fluorine treatment.

FTIR Study of the Acidic Centers

The spectra of Y(28), smY(28), and ssY(28) zeolites are shown in Fig. 2. The OH-region of the normal Y(28) is characterized by bands at 3745, 3632, 3550, and a

TABLE 3

Framework Al Content and Hexane Cracking Activity of the Zeolite Samples before and after Fluorine Treatment

Catalyst	Al _f /u.c. ^a		Activity ^b	
	Before	After ^c	Before	After ^c
Y(54)	54	—	12	24
Y(39)	39	—	27	56
Y(28)	28	—	24	57
Y(26)	26	—	15	35
smY(54)	44	41	127	164
ssY(54)-1	38	35	272	362
ssY(54)-5	21	—	222	248
ssY(39)-1	29	—	382	394
ssY(28)	20	—	431	445

^a Measured by ²⁹Si NMR.

^b μmol/g_{cat.} min.

^c 0.5 g of zeolite was impregnated by 1 ml 0.1 M NH₄F solution.

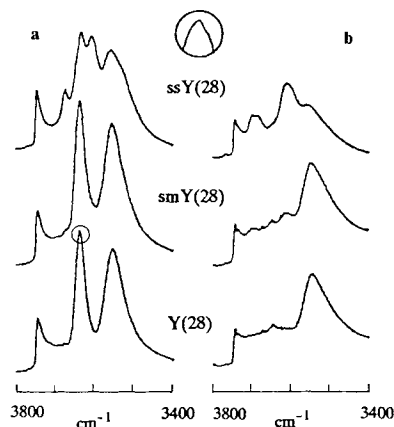


Fig. 2. The IR spectra of the OH-region in the normal, mildly steamed, and severely steamed Y(28) zeolites (a) after evacuation at 400°C and (b) after pyridine adsorption and evacuation at 250°C.

shoulder at 3738 cm^{-1} (Fig. 2a.). The band at 3745 and the shoulder at 3738 cm^{-1} have been assigned to terminal silanol groups and to internal silanols, respectively, arising from incomplete substitution of silicon during treatment with AHFS (12). The bands at 3632 and 3550 cm^{-1} are associated with bridging hydroxyl groups located in the large cages or the small sodalite cages of the Y-type zeolite, respectively. A small additional band was observed in the mildly steamed smY(28) zeolite around 3670 cm^{-1} and the valley was greater between the 3632 and 3550 cm^{-1} peaks. The band at 3632 cm^{-1} , both in the Y(28) and the smY(28) zeolites, actually consists of two bands: a slight shoulder can be observed at 3625 cm^{-1} (see the insert in Fig. 2.). This band can be assigned to another type of bridging hydroxyl group located in the large cages (12), in agreement with the fact that there are two types of framework oxygen in the large cages.

In the severely steamed catalysts (ssY(28)) the spectrum of the OH-region became more complicated. An increase was observed in the band at 3670 cm^{-1} , which has been assigned to the OH-groups connected to extraframework Al species in the

large cages (13, 14). The ssY(28) sample also exhibited a band at 3602 cm^{-1} and a clearly visible shoulder at 3525 cm^{-1} . These bands can be assigned to large and small cage hydroxyl groups, respectively, that are under the influence of cationic extraframework Al species (4, 13, 14).

After pyridine adsorption about half of the sodalite cage OH-groups did not react with pyridine, probably because of steric reasons (Fig. 2b.). The most prominent band that remained was the one at 3550 cm^{-1} . In the ssY(28) zeolite a band at 3612 cm^{-1} also remained. The band observed at 3602 cm^{-1} before pyridine adsorption was superimposed on this band. An additional band appeared at 3690 cm^{-1} after pyridine interaction. A similar band was observed in steamed zeolite-Y after Na^+ poisoning and was attributed to the interaction of the Na^+ cation with residual water (13, 15). Parallel with the appearance of the band at 3690 cm^{-1} the intensity of the 3670 cm^{-1} band decreased. When the pyridine desorption temperature was increased to 400°C, the intensity of the 3690 cm^{-1} band decreased while the intensity of the 3670 cm^{-1} band increased again (not shown in the figure). Hence, the appearance of the band at 3690 cm^{-1} is associated with the interaction of the OH-groups on extraframework Al species with adsorbed pyridine.

Difference spectra shown in Figs. 3a and b were obtained by first recording the spectra of the Y(28) zeolites in the OH-region after activation at 400°C and then subtracting from them the spectra after pyridine adsorption and evacuation at either 250 or 400°C. The difference spectra obtained in this manner reflect the OH bands that react most strongly with pyridine. In the Y(28) and smY(28) zeolites the OH-bands that continue to interact with pyridine following evacuation at 250°C were at 3632 cm^{-1} , and at 3555 cm^{-1} with a shoulder at 3625 cm^{-1} . In the severely steamed sample the band at 3602 cm^{-1} and a shoulder at 3525 cm^{-1} were also involved in pyridine interaction. The band at 3670 cm^{-1} likewise seems to interact

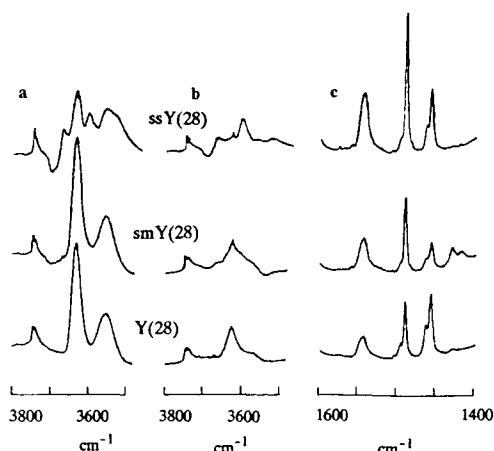


FIG. 3. The difference spectra of the OH-region and the pyridine region in the AHFS-dealuminated, mildly steamed, and severely steamed Y(28) zeolites: (a) the difference spectra in the OH-region for a sample before and after pyridine adsorption and evacuation at 250°C; (b) same as (a) but the spectra after pyridine adsorption and evacuation at 400°C was subtracted; (c) the pyridine region after pyridine adsorption and evacuation at 400°C.

with pyridine; however, a valley can be seen beside this peak under the baseline with a similar negative intensity, so the appearance of this peak on the difference spectrum is attributed to the formation of a new peak at 3690 cm^{-1} and the parallel decrease of the 3670 cm^{-1} band. The terminal and internal silanol groups around 3745 cm^{-1} seem to be involved in the pyridine interaction; however, these OH-groups are nonacidic and can interact with a base such as pyridine only by hydrogen bonding (16). After evacuation at 400°C only a few remaining bands interact with pyridine. In Y(28) the band at 3632 cm^{-1} remains; in smY(28) the band at 3625 cm^{-1} and a shoulder at 3602 cm^{-1} remain; in ssY(28) a weak band at 3625 cm^{-1} , the band at 3602 cm^{-1} , and a weak band at 3525 cm^{-1} can be observed.

After evacuation at 400°C the intensity of the band at 1545 cm^{-1} , assigned to pyridinium cations formed on Brønsted acidic centers, increased after mild or severe steaming (Fig. 3c), showing that the concentration of

the strongly acidic sites increased. The two peaks around 1456–1462 cm^{-1} were assigned to pyridine coordinatively bonded to Lewis acidic sites. The Y(28) zeolite exhibited many more of these Lewis acidic sites than expected. Probably some extraframework Al species were formed either during treatment with AHFS or during the activation in N_2 and evacuation at 400°C; however, they did not influence the concentration of strong Brønsted acidic sites. Moreover, no additional bands were observed in the OH-region, unlike in the severely steamed sample (ssY(28)) for which the deposited extraframework Al had a large effect on the OH region. These unexpected Lewis-sites in the Y(28) sample probably are not inside the pores of the zeolite.

MAS NMR Study

The results of ^{29}Si NMR measurements are summarized in Table 4. The symbols Si(3), Si(2), Si(1), Si(0) correspond to Si atoms connected to 3, 2, 1, or 0 Al_f atoms. An additional broad peak was observed around -110 ppm in the spectra of Y(26) zeolites which had about 50% crystallinity. This resonance probably results from the Si in the amorphous silica-alumina phase. After AHFS treatment the number of Si atoms connected to two Al atoms in the lattice decreased with decreasing framework Al content (series a) while the number of Si(1) atoms remained constant and the number of Si(0) atoms increased. After mild or severe steaming both the number of Si(2) and Si(1) atoms decreased (series b and c), except for the Y(39) zeolite, which did not show any significant decrease in the Si(1) resonance. Similarly, a decrease in the Si(3) and Si(2) resonances was observed in the mild and severely steamed parent catalyst series (series e and f).

The ^{29}Si spectra of Y(39) and ssY(54)-1 samples having the same Al_f content per u.c. are shown in Fig. 4. After AHFS dealumination of the parent Y(54) zeolite no Si(3) atoms were detected, but when the parent catalyst was dealuminated by steaming to

TABLE 4
Framework/Nonframework Al Content and Si
Distribution in the Zeolite Samples

Zeolite	Unit cell					
	Al _f	Al _{nf}	Si(0)	Si(1)	Si(2)	Si(3)
Y(39) ^a	39	—	42	69	45	—
Y(30)	30	—	66	73	23	—
Y(28)	28	—	72	72	20	—
Y(26)	26	—	81	69	16	—
smY(39) ^b	34	5	54	72	32	—
smY(28)	26	2	81	68	17	—
smY(30)	24	6	84	68	16	—
smY(26)	23	3	91	62	16	—
ssY(39)-1 ^c	29	10	75	67	21	—
ssY(28)	20	8	104	58	10	—
ssY(30)-1	16	14	123	43	10	—
ssY(30)-2	13	17	133	38	8	—
ssY(26)	20	6	107	51	13	—
Y(54) ^d	54	—	14	49	57	18
smY(54) ^e	43	11	33	68	39	8
ssY(54)-1 ^f	38	16	52	66	26	10
ssY(54)-2	32	22	68	62	22	8
ssY(54)-3	29	25	83	52	19	8
ssY(54)-4	27	27	—	—	—	—
ssY(54)-5	21	33	—	—	—	—
smY(54)/F ^g	41	13	41	66	36	9
ssY(54)-1/F	35	19	59	66	23	9

^a Prepared from the parent Y(54) zeolite by AHFS treatment.

^b AHFS-treated series after mild steaming.

^c AHFS-treated series after severe steaming.

^d Parent zeolite.

^e Mild steamed parent zeolite.

^f Severely steamed parent zeolite series.

^g Fluorine-treated samples.

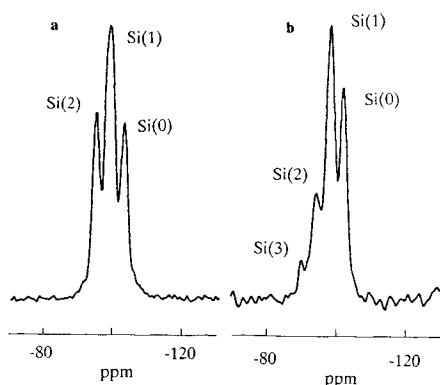


FIG. 4. The ²⁹Si spectra of (a) Y(39) zeolite prepared by AHFS-modification, and (b) ssY(54)-1 zeolite prepared by severe steaming of the parent zeolite to a level of 38 Al_f/u.c.

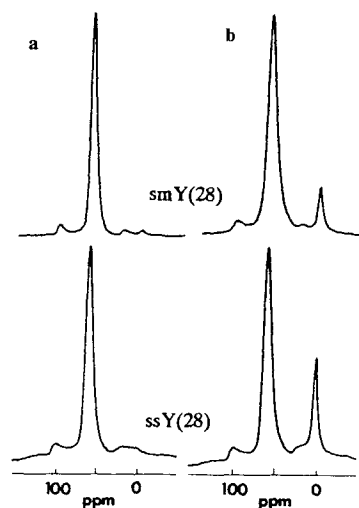


FIG. 5. The ²⁷Al spectra of the smY(28) and ssY(28) samples in (a) NH₄⁺-form and (b) H⁺-form.

the same Al_f content, a considerable amount of Si(3) atoms remained in the sample.

The ²⁷Al spectra of smY(28) and ssY(28) samples are shown in Fig. 5. Based on the results of Table 1 one would expect the ssY(28) sample to have hexagonally coordinated Al which would give a resonance around 0 ppm. As shown in Fig. 5, a strong resonance at 59 ppm due to tetrahedral Al was observed, but the resonance at 0 ppm was very small. After activation at 400°C in flowing N₂ the peak assigned to hexagonally coordinated extraframework Al species around 0 ppm became apparent. Moreover, there was a good agreement between the framework/nonframework Al ratios calculated from the ²⁹Si and ²⁷Al spectra. The ratios were 12 and 12.5 in smY(28) based on ²⁹Si and ²⁷Al data, respectively, and 2.8 and 3.2 in ssY(28). It should be noted that a Y(28) sample activated at 400°C in N₂, but without steaming also exhibited a resonance at 0 ppm.

From the spectra of Fig. 5 the only apparent form of extraframework aluminum was hexagonally coordinated; however, when the spectrum was obtained with a 400 MHz instrument and the sample was spun at 7

kHz, a broad resonance centered at ca. 50 ppm was clearly evident in the ssY(28) sample. This resonance was not observed with the Y(28) zeolite. The resonance at 50 ppm has been assigned to a nonframework tetrahedral form of aluminum (4, 17). The area under the broad resonance is approximately 20% of the total tetrahedral resonance, which corresponds to 5.6 Al/u.c.

DISCUSSION

The catalytic results obtained on the H-Y catalyst series prepared by AHFS modification are in a good agreement with those obtained in previous studies (3, 6). The activities of these materials were quite small, which supports the hypothesis that the presence of isolated Al_f atoms is a necessary but not sufficient condition for achieving high acidity. When these zeolites were steamed to a level of only about one extraframework Al atom per β -cage, their activity reached a maximum value. Presumably, the presence of a small amount of cationic aluminum greatly increased the acidity of certain protons in the zeolite. The activities achieved were significantly greater than the maximum activity of the steamed parent Y(54) zeolite.

The ^{29}Si results show that in the steamed parent zeolites (series e and f in Table 4.) the concentration of those Si atoms which were connected to 3, 2, or 1 Al_f atoms generally decreased in a parallel manner, while the concentration of Si(0) atoms increased continuously. In addition, each type of Si atom (i.e., those connected to 0, 1, 2, or 3 Al_f atoms) was present in the zeolite even at the lower Al_f content. In the case of Si(2) atoms one could imagine an Al_f distribution where the two Al_f atoms are present in two different four-rings, but the presence of Si(3) centers implies that two Al_f atoms are in a single four-ring. The protons associated with hydroxyl groups in such four-rings would not be strongly acidic. We conclude, therefore, that in the steamed parent zeolite series not all the framework Al atoms are isolated and related to strong acidity even when the Al_f content is ≤ 32 per u.c. The

fact that Si(3) is not zero indicates that N(0) is not the only form of Al_f at ≤ 32 per unit cell. This means that zeolites prepared by steam dealumination do not strictly obey the significant structures model (11), even though the sharp maximum in activity at 32 Al_f /u.c. is in agreement with this model.

The advantage of the AHFS dealumination is clearly seen from the results shown in Table 4. When the Al_f content of the parent catalyst was reduced from 54 to 39 by AHFS treatment, those Al_f atoms were eliminated selectively by Si substitution which had a next nearest neighbors in the four-rings; no Si(3) atoms were detected in the Y(39) sample (see also Fig. 4.). At increasing dealumination levels the number of Si(1) atoms remained constant (ca. 70), while the number of Si(2) atoms decreased (series a). Probably the AHFS treatment removed those Al_f atoms from the zeolite which were bonded less strongly to the lattice, i.e., those Al_f atoms which were in a less silicious environment. The steam dealumination seems to be less selective, perhaps because of the high dealumination temperature (550–600°C) applied during the steaming procedure.

The observed selectivity during AHFS dealumination has an important consequence in that the samples prepared by this method have a higher concentration of isolated framework Al atoms relative to zeolite prepared by steaming the parent Y(54) zeolite. This difference may manifest itself in the higher hexane cracking activities reached on severely steamed AHFS-treated samples (Fig. 1). In a recent study in our laboratory (4), higher hexane cracking activities were observed on the steamed H-ZSM-20 catalysts relatively to the steamed H-Y zeolites. In this study the parent ZSM-20 catalysts contained 42 Al_f /u.c. and no Si(3) peak was observed on the ^{29}Si spectrum. Over 400 $\mu\text{mol/g}_{\text{Cat}}$ min hexane cracking activity was reached, and the maximum was positioned around 32 Al_f /u.c. In our case, when the Y(39) catalyst (39 Al_f /u.c.) containing a certain amount of isolated Al_f atoms was steamed to different levels (i.e., the complete

activity curve was measured, as shown in Fig. 1), an activity curve very similar to that found for H-ZSM-20 was observed.

The AHFS-modified catalysts contained less extraframework Al species after steaming than the steamed parent catalysts (Table 4), but they showed similar or even greater hexane cracking activity. For example the activities of the mildly steamed samples (series b) were only about 10–25% less than the activities of the steamed parent catalyst series, although these samples contained only around 3–6 extraframework Al atoms per unit cell which may be compared with 10–30 extraframework Al atoms in the steamed parent catalysts. As noted above, the number of isolated Al_f atoms is probably higher in the AHFS-modified samples relative to the parent catalyst before steaming. Furthermore, the amount and distribution of the essential cationic form of extraframework Al may be closer to the optimum in the AHFS-modified samples. In the AHFS-modified samples a larger fraction of the extraframework Al species seems to be effective for increasing the acidic strength of the Brønsted centers.

By increasing severity of the steaming the OH-bands taking part in the interaction with pyridine at 400°C (i.e., the strongest acidic sites) shifted to lower wavenumbers, showing the increasing acidity of the protons (Fig. 3b). In the unsteamed H-Y(28) sample some of the large cage OH-groups (at 3632 cm^{-1} and a shoulder at 3625 cm^{-1}) interact with pyridine even after treatment at 400°C. In the mildly steamed sample (smY(28)) a shoulder at 3602 cm^{-1} was observed in addition to the band at 3632 cm^{-1} . After severe steaming (ssY(28)) the 3602 cm^{-1} band dominated the spectrum, but the band at 3525 cm^{-1} indicates that the strongly acid OH-groups in the β -cages also took part in the interaction with pyridine (13, 18). The pyridine molecule is too large to enter into the small cages, but the mobility of the proton makes possible the formation of a pyridinium ion.

A pair of bands at 3602 and 3526 cm^{-1}

also was observed following the activation of H-ZSM-20 by steaming (4). These bands were affected more strongly by the addition of Na^+ than were the less acidic bands 3624 and 3550 cm^{-1} . It should be noted from the spectra of Fig. 3a that even after severe steaming the hydroxyl groups characterized by the bands at 3602 and 3526 cm^{-1} constitute only a fraction of those present in the zeolite. Thus, dealumination decreases the total number of acid protons in the zeolite, but upon subsequent steaming some of these become strongly acidic.

By analogy with the positive effect of La^{3+} ions on acidity (3), we propose that cationic tetrahedral Al is present in the β -cages as $Al(OH)^{2+}$ species. This tetrahedral form of Al is believed to be responsible for the resonance at 50 ppm. Through inductive effects this cationic Al species withdraws electrons from OH-bonds, thus making the protons more acidic.

For sake of illustration consider a zeolite in which there are 24 $Al_f/u.c.$ and 4 $Al(OH)^{2+}/u.c.$ On the average there would be 3 Al_f/β -cage and 0.5 $Al(OH)^{2+}/\beta$ -cage. In half the β -cages an $Al(OH)^{2+}$ cation would charge compensate two Al_f tetrahedra, and there would be one strongly acidic proton. In each of the remaining β -cages there would be three weakly acidic protons. The relative number of strongly and weakly acidic protons is consistent with the amplitudes of the 3602 and 3525- cm^{-1} hydroxyl bands. At higher $Al_f/u.c.$ concentrations charge compensation by $Al(OH)^{2+}$ is not a problem, but at lower Al_f concentrations and higher cationic extraframework Al concentrations no protons would be needed. But since only a fraction of the extraframework species are cationic, in the severely steamed samples with lower Al_f content a delocalization of charge over rather long distance must take place (4). That is, a multivalent extraframework Al species will influence not only those protons in its immediate vicinity, but also those which are in other adjacent small cages and hexagonal prisms.

It should be noted that the hexagonally

coordinated extraframework Al species remained "NMR invisible" in the NH_4^+ -ion exchanged samples (Fig. 5a) and became "visible" after activation in N_2 at 400°C . Klinowski *et al.* (19) have found a large disagreement between the $\text{Al}_f/\text{Al}_{\text{nf}}$ ratios determined from the ^{29}Si and ^{27}Al spectra of a series of steam-dealuminated Y-zeolite. Their samples were NH_4^+ -ion exchanged after steaming but before the NMR measurements. $\text{Al}(\text{OH})_3$, $\text{Al}(\text{OH})^{2+}$, Al_2O_3 , and some polymeric Al species were suggested as the possible forms of the "invisible" extraframework Al. When the dealumination was carried out by SiCl_4 treatment, much better agreement was found between the ^{29}Si and ^{27}Al NMR results. They concluded that dealumination with SiCl_4 produced fewer immobile aluminum complexes, not observable by NMR; however, in this later experiment the Na^+ -form of the Y-zeolite was used.

In our case the AHFS-modified and then steamed samples were also NH_4^+ -ion exchanged before the ^{29}Si NMR measurements. The octahedral extraframework Al species became "visible" only after the samples were activated in N_2 at 400°C . It is clear from the data of Table 1 that extraframework Al species in the ssY(28) sample were formed during the AHFS treatment and steaming at 550 or 600°C , rather than during the activation in N_2 at 400°C . From our results we suggest that in the NH_4^+ form of the dealuminated Y-zeolite the octahedral symmetry of the extraframework Al might be altered, thus making them "NMR invisible." With the zeolite in the H^+ -form after activation the symmetry of this species was restored, and the agreement between the concentrations of extraframework Al as determined from the ^{29}Si and ^{27}Al spectra became much better.

The fluorine treatment had some beneficial effect on the zeolite acidity and activity. This activity increase can be attributed mainly to the formation of additional extraframework Al species during the fluorine treatment. The NH_4F introduced into the

zeolite by impregnation decomposes at elevated activation temperature (up to 400°C) and HF is formed. The HF might cause dealumination (20).

Becker and Kowalak (21) have observed a significant increase in the acidity and catalytic activity of high-silica mordenite and ZSM-5 catalysts upon fluorine treatment (their samples were impregnated by NH_4F and activated at an elevated temperature); however, significant framework dealumination was always detected. In addition, they observed a similar increase in activity in Al^{3+} ion-exchanged Y-zeolites after fluorine treatment (22). The interpretation of this results is complicated by the fact that dealumination was observed, and the zeolites contained a significant Na^+ -ion concentration which decreased with the severity of the fluorine treatment. In both cases the increased acidity and activity were attributed to the formation of Al-F species which, acting as strong Lewis acidic sites, interact with acidic OH-groups.

In our case, very little fluorine remained in the samples, and this was probably in the form proposed by Becker and Kowalak. Although this fluorine may have a small direct effect on acidity, it seems that the increase in activity can largely be explained by an increase in the extent of dealumination. The exception would be the ssY(54)-5 sample, for which a greater extent of dealumination would be expected to reduce the activity. In fact, treatment with NH_4F increased the activity about 10%.

CONCLUSIONS

An AHFS treatment selectively removes those Al_f atoms which have second nearest tetrahedral Al_f neighbors in the four-rings, but the resulting zeolite is relatively inactive for hexane cracking. Subsequent steaming is a necessary step for producing extraframework Al species in the zeolite which enhance the acidity of the protons associated with isolated Al_f atoms. Steaming removes the Al_f atoms from the lattice in a random manner. The enhanced activity of

the steamed AHFS-modified samples, relative to the steamed parent catalysts, can be attributed to the larger amount of the isolated Al_i atoms in this zeolite and a more favorable extraframework Al concentration and distribution.

The strongest acidic centers can be attributed to the presence of the OH-bands at 3602 and 3625 cm⁻¹, which were assigned to large and small cage OH-groups, respectively, in the presence of extraframework Al species. Only a fraction of the extraframework Al species seems to be effective for increasing acidity in the steamed AHFS-modified catalysts. If a way could be found to introduce this form of extraframework Al as a separate step, it should be possible to produce an even more active catalyst than that prepared in this study.

The activity increase observed after slight fluorine treatment can be attributed mainly to the dealumination caused by HF formed from NH₄F during the activation at 400°C. The presence of fluorine in the zeolites after AHFS treatment is believed to play only a minor role in effecting strong acidity.

ACKNOWLEDGMENTS

This research was supported by the State of Texas Advanced Technology Program. We are indebted to Dr. P.-J. Chu and Dr. G. J. Ray for their help in obtaining the NMR spectra.

REFERENCES

1. DeCanio, S. J., Sohn, J. R., Fritz, P. O., and Lunsford, J. H., *J. Catal.* **101**, 132 (1986).
2. Sohn, J. R., DeCanio, S. J., Fritz, P. O., and Lunsford, J. H., *J. Phys. Chem.* **90**, 4847 (1986).
3. Carvajal, R., Chu, P.-J., and Lunsford, J. H., *J. Catal.* **125**, 123 (1990).
4. Sun, Y., Chu, P.-J., and Lunsford, J. H., *Langmuir* **7**, 3027 (1991).
5. Skeels, G. W., and Breck, D. W., in "Proceedings, 6th International Conference" (D. Olson and A. Bisio, Eds.), p. 87. Butterworths, Guilford, 1984.
6. Beyerlein, R. A., McVicker, G. B., Yacullo, L. N., and Ziemiak, J. J., *J. Phys. Chem.* **92**, 1967 (1988).
7. Pellet, R. J., Blackwell, C. S., and Rabo, J. A., *J. Catal.* **114**, 71 (1988).
8. Troll, G., Farzaneh, A., and Gammann, K., *Chem. Geol.* **20**, 295 (1977).
9. Sohn, J. R., DeCanio, S. J., Lunsford, J. H., and O'Donnell, D. J., *Zeolites* **6**, 225 (1986).
10. Engelhardt, G., Lohse, V., Lippmaa, E., Tarnak, M., and Magi, M., *Z. Anorg. Allg. Chem.* **482**, 49 (1981).
11. Beagley, B., Dwyer, J., Fitch, F. R., Mann, R., and Walters, J., *J. Phys. Chem.* **88**, 1744 (1984).
12. Dwyer, J., Dewing, J., Thompson, N. E., O'Malley, P. J., and Karim, K., *J. Chem. Soc., Chem. Commun.*, 843 (1989).
13. Fritz, P. O., and Lunsford, J. H., *J. Catal.* **118**, 85 (1989).
14. Corma, A., Fornes, V., and Rey, F., *Appl. Catal.* **59**, 267 (1990).
15. Ward, J. W., in "Zeolite Chemistry & Catalysis" (J. A. Rabo, Ed.), p. 187. American Chemical Society, Washington, DC, 1976.
16. Karge, H., *Z. Phys. Chem.* **80**, 60 (1976).
17. Samoson, A., Lippmaa, E., Engelhardt, G., Lohse, V., and Jerschke, H.-G., *Chem. Phys. Lett.* **134**, 589 (1987).
18. Lombardo, E. A., Sill, G. A., and Hall, W. K., *J. Catal.* **119**, 426 (1989).
19. Klinowski, J., Fyfe, C. A., and Gobbi, G. C., *J. Chem. Soc. Faraday Trans. 1* **81**, 3003 (1985).
20. Wang, Q. L., Giannetto, G., and Guisnet, M., *Zeolites* **10**, 301 (1990).
21. Becker, K. A., and Kowalak, S., in "Recent Advances in Zeolite Science" (J. Klinowski and P. Barrie, Eds.), Studies in Surface Science and Catalysis, Vol. 52, p. 123. Elsevier, Amsterdam, 1989.
22. Becker, K. A., and Kowalak, S., *J. Chem. Soc. Faraday Trans. 1* **83**, 535 (1987).